

MATRIX-FREE CONSTRUCTION OF HSS REPRESENTATION USING ADAPTIVE RANDOMIZED SAMPLING

CHRISTOPHER GORMAN*, GUSTAVO CHÁVEZ†, PIETER GHYSELS†, THÉO MARY‡,
FRANÇOIS-HENRY ROUET§, AND XIAOYE SHERRY LI†

Abstract. We present new algorithms for randomized construction of hierarchically semi-separable matrices, addressing several practical issues. The HSS construction algorithms use a partially matrix-free, adaptive randomized projection scheme to determine the maximum off-diagonal block rank. We develop both relative and absolute stopping criteria to determine the minimum dimension of the random projection matrix that is sufficient for desired accuracy. Two strategies are discussed to adaptively enlarge the random sample matrix: repeated doubling of the number of random vectors, and iteratively incrementing the number of random vectors by a fixed number. The relative and absolute stopping criteria are based on probabilistic bounds for the Frobenius norm of the random projection of the Hankel blocks of the input matrix. We discuss parallel implementation and computation and communication cost of both variants. Parallel numerical results for a range of applications, including boundary element method matrices and quantum chemistry Toeplitz matrices, show the effectiveness, scalability and numerical robustness of the proposed algorithms.

Key word. Hierarchically Semi-Separable, randomized sampling, randomized projection

1. Introduction. Randomization schemes have proven to be a powerful tool for computing a low-rank approximation of a dense matrix, or as we call it in this work, *compressing* it. The main advantage of randomization is that these methods usually require fewer computations and communication than their traditional deterministic counterparts, resulting in large savings in terms of memory and floating point operations.

For classes of dense matrices that have off-diagonal blocks that can be approximated as low-rank submatrices, randomized methods are particularly advantageous. These matrices are referred to as *structured*, and there are many types of matrix formats that can take advantage of this structure; these include, to name a few, Hierarchically Semi-Separable (HSS) matrices [3], \mathcal{H} and \mathcal{H}^2 matrices [9, 8]. This work focuses on HSS representations, and more specifically on efficient HSS compression. HSS compression is the central component of the HSS framework; once a matrix is compressed into its HSS form, one can take advantage of fast algorithms for multiplication, factorization, . . .

One way to speedup HSS compression involves using randomization [12, 10]. Randomization involves generating *samples* of size at least the maximum rank of the HSS representation. Since the exact rank of low-rank matrices is usually not known in practice, adaptive algorithms are needed in order to generate sufficient, yet not too many, random samples, until the range is well approximated and the matrix is compressed to a desired tolerance. This ensures robustness and high performance of the overall algorithm.

This paper builds on our previous work [14], which gives an explicit adaptive algorithm. One of the highlights of this work is the development of a new stopping criterion that considers both relative and absolute error. We demonstrate the effectiveness of this novel approach, and others, in a set of numerical experiments that showcase the scalability and robustness of the new algorithms on a variety of matrices

*University of California, Santa Barbara, Santa Barbara, CA, USA. gorman@math.ucsb.edu

†Lawrence Berkeley National Laboratory, Berkeley, CA, USA. {gichavez,pghysels,xsli}@lbl.gov

‡University of Manchester, Manchester, UK. theo.mary@manchester.ac.uk

§Livermore Software Technology Corporation, Livermore, CA, USA. frouet@lsc.com

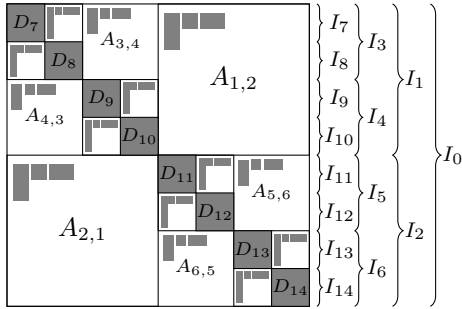


FIG. 1. Illustration of an HSS matrix using 4 levels. Diagonal blocks are partitioned recursively. Gray blocks denote the basis matrices.

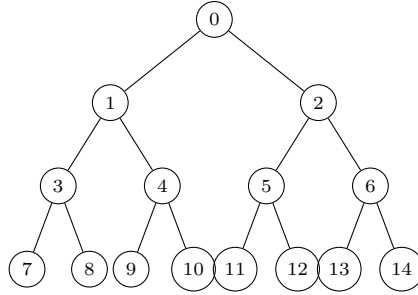


FIG. 2. Tree for Figure 1, using level-by-level top-down numbering. All nodes except the root store U_μ and V_μ . Leaves store D_μ , non-leaves B_{ν_1, ν_2} , B_{ν_2, ν_1}

from different applications.

The paper is organized as follows. In Section 2, we discuss the HSS randomized construction algorithm, the two adaptive sampling strategies, and the new stopping criterion for terminating adaptation. The parallel algorithms are presented and analyzed in Section 3, followed by numerical experiments in Section 4. The probability theory proofs necessary for our new stopping criterion are relegated to Appendix A.

2. Hierarchically Semi-Separable Matrices and Randomized Construction . In Section 2.1, we briefly describe the HSS matrix format. Section 2.2 outlines the randomized HSS construction scheme from [12]. Section 2.4 introduces two new schemes that can be used to adaptively determine the maximum HSS rank, making the randomized HSS construction more robust. The final sections discuss the derivation of the stopping criteria used in the adaptive schemes.

2.1. HSS Representation. This short HSS introduction mostly follows the notation from [12]. For a more detailed description of the HSS matrix format, as well as for fast HSS algorithms, we refer the reader to the standard HSS references [3, 20].

The following notation is used: ‘:’ is matlab-like notation for all indices in the range, * denotes complex conjugation, $\#I_\tau$ is the number of elements in index set $I_\tau = \{i_1, i_2, \dots, i_n\}$, $R_\tau = R(I_\tau, :)$ is the matrix consisting of only the rows I_τ of matrix R and $I_\tau \setminus I_\nu$ is the set of indices in I_τ minus those in I_ν .

Consider a square matrix $A \in \mathbb{C}^{N \times N}$ with an index set $I_A = \{1, \dots, N\}$ associated with it. Let \mathcal{T} be a binary tree, ordered level by level, starting with zero at the root node. Each node τ of the tree is associated with a contiguous subset $I_\tau \subset \mathcal{I}$. For two siblings in the tree, ν_1 and ν_2 , children of τ , it holds that $I_{\nu_1} \cup I_{\nu_2} = I_\tau$ and $I_{\nu_1} \cap I_{\nu_2} = \emptyset$. It follows that $\cup_{\tau=\text{leaves}(\mathcal{T})} I_\tau = I_{\text{root}(\mathcal{T})} = I_A$. The same tree \mathcal{T} is used for the rows and the columns of A and only diagonal blocks are partitioned. An example of the resulting matrix partitioning is given in Figure 1 and the corresponding tree is shown in Figure 2.

The diagonal blocks of A , denoted D_τ , are stored as dense matrices in the leaves τ of the tree \mathcal{T}

$$(2.1) \quad D_\tau = A(I_\tau, I_\tau).$$

The off-diagonal blocks $A_{\nu_1, \nu_2} = A(I_{\nu_1}, I_{\nu_2})$, where ν_1 and ν_2 denote two siblings in

the tree, are factored (approximately) as

$$(2.2) \quad A_{\nu_1, \nu_2} \approx U_{\nu_1}^{\text{big}} B_{\nu_1, \nu_2} (V_{\nu_2}^{\text{big}})^*.$$

The matrices $U_{\nu_1}^{\text{big}}$ and $V_{\nu_2}^{\text{big}}$, which form bases for the column and row spaces of A_{ν_1, ν_2} , are typically tall and skinny, with $U_{\nu_1}^{\text{big}}$ having $\#I_{\nu_1}$ rows and $r_{\nu_1}^r$ (column-rank) columns, $V_{\nu_2}^{\text{big}}$ has $\#I_{\nu_2}$ rows and $r_{\nu_2}^c$ (row-rank) columns and hence B_{ν_1, ν_2} is $r_{\nu_1}^r \times r_{\nu_2}^c$. The HSS-rank r of matrix A is defined as the maximum of $r_{\nu_1}^r$ and $r_{\nu_2}^c$ over all off-diagonal blocks, where typically $r \ll N$. The matrices B_{ν_1, ν_2} and B_{ν_2, ν_1} are stored in the parent of ν_1 and ν_2 . For a non-leaf node τ with children ν_1 and ν_2 , the basis matrices $U_{\nu_1}^{\text{big}}$ and $V_{\nu_2}^{\text{big}}$ are not stored directly since they can be represented hierarchically as

$$(2.3) \quad U_{\tau}^{\text{big}} = \begin{bmatrix} U_{\nu_1}^{\text{big}} & 0 \\ 0 & U_{\nu_2}^{\text{big}} \end{bmatrix} U_{\tau} \quad \text{and} \quad V_{\tau}^{\text{big}} = \begin{bmatrix} V_{\nu_1}^{\text{big}} & 0 \\ 0 & V_{\nu_2}^{\text{big}} \end{bmatrix} V_{\tau}.$$

Note that for a leaf node $U_{\tau}^{\text{big}} = U_{\tau}$ and $V_{\tau}^{\text{big}} = V_{\tau}$. Hence, every node τ with children ν_1 and ν_2 , except for the root node, keeps matrices U_{τ} and V_{τ} . For example, the top two levels of the example shown in Figure 1 can be written out explicitly as

$$(2.4) \quad A = \begin{bmatrix} D_3 & U_3 B_{3,4} V_4^* & \begin{bmatrix} U_3 & 0 \\ 0 & U_4 \end{bmatrix} U_1 B_{1,2} V_2^* \begin{bmatrix} V_5^* & 0 \\ 0 & V_6^* \end{bmatrix} \\ U_4 B_{4,3} V_3^* & D_4 & \\ \begin{bmatrix} U_5 & 0 \\ 0 & U_6 \end{bmatrix} U_2 B_{2,1} V_1^* \begin{bmatrix} V_3^* & 0 \\ 0 & V_4^* \end{bmatrix} & D_5 & U_5 B_{5,6} V_6^* \\ & U_6 B_{6,5} V_5^* & D_6 \end{bmatrix}.$$

The storage requirement for an HSS matrix is $\mathcal{O}(rN)$. Construction of the HSS generators will be discussed in the next section. Once an HSS representation of a matrix is available, it can be used to perform matrix-vector multiplication in $\mathcal{O}(rN)$ operations compared to $\mathcal{O}(N^2)$ for classical dense matrix-vector multiplication, see [12, 14].

2.2. Randomized HSS Construction. Here we review the randomized HSS construction algorithm as presented by Martinsson [12] as well as the adaptive variant as described in [14, 6, 5]. This algorithm requires matrix vector products, for the random sampling, as well as access to certain entries of the input matrix, for construction of the diagonal blocks D_i and the B_{ij} generators. We therefore refer to it as “partially matrix-free”. A fully matrix-free randomized HSS compression algorithm was presented in [11], which does not require access to individual matrix elements, but requires $\mathcal{O}(\log N)$ more random projection vectors instead of requiring access to $\mathcal{O}(rN)$ matrix elements.

Let us assume for now that the maximum rank encountered in any of the HSS off-diagonal blocks is known to be r . Let R be an $N \times d$ random matrix, where $d = r + p$ with p a small oversampling parameter. The matrix U_{τ} in the HSS representation is a basis for the column space of the off-diagonal row block $A(I_{\tau}, I_A \setminus I_{\tau})$. Likewise, V_{τ} is a basis for the row space of $A(I_A \setminus I_{\tau}, I_{\tau})^*$. These row and column off-diagonal blocks are called Hankel blocks. In order to compute the random projection of these Hankel blocks, we first compute both $S^r = AR$ and $S^c = A^*R$, such that $S^r(I_{\tau}, :)$ is the random projection of the entire row block $A(I_{\tau}, :)$. Let D_{τ} for non-leaf nodes be defined (recursively) as $D_{\tau} = \begin{bmatrix} D_{\nu_1} & A_{\nu_1, \nu_2} \\ A_{\nu_2, \nu_1} & D_{\nu_2} \end{bmatrix}$, and with nodes τ_i, \dots, τ_j on level ℓ of the HSS tree, we define the block diagonal matrix $D^{(\ell)} = \text{diag}(D_{\tau_i}, \dots, D_{\tau_j})$. At each level of the HSS tree we can compute the samples of the Hankel blocks as

$$(2.5) \quad S^{r,(\ell)} = (A - D^{(\ell)})R = S^r - D^{(\ell)}R \quad \text{and} \quad S^{c,(\ell)} = S^c - D^{(\ell)*}R.$$

By starting from the leaf level of the HSS tree and working up towards the root, this calculation can be performed efficiently, since the off-diagonal blocks of D_τ are already compressed. Consider a leaf node τ , and let $S_\tau^r = S^r(I_\tau, :) - D_\tau R(I_\tau, :)$. To compute the U_τ basis from this random projection matrix, an interpolative decomposition (ID) is used, which expresses the matrix S_τ^r as a linear combination of a selected set J_τ^r of its rows $S_\tau^r = U_\tau S_\tau^r(J_\tau^r, :) + \mathcal{O}(\varepsilon)$, where $\#J_\tau^r$ is the ε -rank of S_τ^r . This decomposition can be computed using a rank-revealing QR factorization, or QR with column pivoting (QRCP), applied to $(S_\tau^r)^*$ as follows:

$$(2.6) \quad (S_\tau^r)^* \approx Q [R_1 \quad R_2] \Pi^T = (QR_1) [I \quad R_1^{-1} R_2] \Pi^T$$

$$(2.7) \quad \approx (S_\tau^r(J_\tau^r, :))^* [I \quad R_1^{-1} R_2] \Pi^T,$$

with Π a permutation matrix moving columns J_τ^r to the front, Q orthogonal and R_1 upper triangular. Note that QRCP selects columns J_τ^r of $(S_\tau^r)^*$, which corresponds to the transposed rows J_τ^r of S_τ^r . From (2.7), U_τ can be defined as

$$(2.8) \quad U_\tau = \Pi \begin{bmatrix} I \\ (R_1^{-1} R_2)^* \end{bmatrix} = \Pi_\tau^r \begin{bmatrix} I \\ E_\tau^r \end{bmatrix},$$

and, likewise $V_\tau = \Pi_\tau^c [I \quad (E_\tau^c)^*]^*$. From these definitions of U_τ and V_τ , we see that if ν_1 and ν_2 are leaf nodes

$$(2.9) \quad A_{\nu_1, \nu_2} \approx U_{\nu_1} B_{\nu_1, \nu_2} (V_{\nu_2})^* = \Pi_\tau^r \begin{bmatrix} I \\ E_\tau^r \end{bmatrix} B_{\nu_1, \nu_2} [I \quad (E_\tau^c)^*] (\Pi_\tau^c)^T$$

and hence $B_{\nu_1, \nu_2} = A_{\nu_1, \nu_2}(J_{\nu_1}^r, J_{\nu_2}^c)$ is a sub-block of A_{ν_1, ν_2} .

Note that Equation (2.5) can be used for the leaf levels. On the higher levels however, we need to guarantee the nested basis property, see Equation (2.3). For a non-leaf node τ with (leaf) children ν_1 and ν_2 we have

$$(2.10) \quad S_\tau^{r,(\ell)} = (A(I_\tau, :) - D_\tau) R = A(I_\tau, :) R - \begin{bmatrix} D_{\nu_1} & A_{\nu_1, \nu_2} \\ A_{\nu_2, \nu_1} & D_{\nu_2} \end{bmatrix} \begin{bmatrix} R(I_{\nu_1}, :) \\ R(I_{\nu_2}, :) \end{bmatrix}$$

$$(2.11) \quad = \begin{bmatrix} S_{\nu_1}^r \\ S_{\nu_2}^r \end{bmatrix} - \begin{bmatrix} & A_{\nu_1, \nu_2} \\ A_{\nu_2, \nu_1} & \end{bmatrix} \begin{bmatrix} R(I_{\nu_1}, :) \\ R(I_{\nu_2}, :) \end{bmatrix}$$

$$(2.12) \quad \approx \begin{bmatrix} U_{\nu_1} S_{\nu_1}^r(J_{\nu_1}^r, :) - U_{\nu_1} B_{\nu_1, \nu_2} V_{\nu_1}^* R(I_{\nu_2}, :) \\ U_{\nu_2} S_{\nu_2}^r(J_{\nu_2}^r, :) - U_{\nu_2} B_{\nu_2, \nu_1} V_{\nu_2}^* R(I_{\nu_1}, :) \end{bmatrix}$$

$$(2.13) \quad \approx \begin{bmatrix} U_{\nu_1} & \\ & U_{\nu_2} \end{bmatrix} \begin{bmatrix} S_{\nu_1}^r(J_{\nu_1}^r, :) - B_{\nu_1, \nu_2} V_{\nu_2}^* R(I_{\nu_2}, :) \\ S_{\nu_2}^r(J_{\nu_2}^r, :) - B_{\nu_2, \nu_1} V_{\nu_1}^* R(I_{\nu_1}, :) \end{bmatrix}.$$

We let $\tau.R^r \leftarrow V_\tau^* R(I_\tau, :)$ and

$$(2.14) \quad \tau.S^r \leftarrow \begin{bmatrix} S_{\nu_1}^r(J_{\nu_1}^r, :) - B_{\nu_1, \nu_2} \nu_2.R \\ S_{\nu_2}^r(J_{\nu_2}^r, :) - B_{\nu_2, \nu_1} \nu_1.R \end{bmatrix},$$

so we can apply ID($\tau.S^r$) in order to compute U_τ , since the U_{ν_1} and U_{ν_2} bases have been factored out in Eq. (2.13). This can be applied recursively to nodes with children that are non-leaf nodes. A similar reasoning also applies for ID($\tau.S^c$).

These steps, Eqs. (2.5)-(2.13), are implemented in Algorithms 1 and 2, with some definitions in Table 1. We use notation like $\tau.J^r$ to denote that the temporary variable J_τ^r is stored at node τ . Algorithm 1 implements the recursive bottom-up HSS tree

Algorithm 1: Non-adaptive HSS compression of $A \in \mathbb{R}^{N \times N}$ using cluster tree \mathcal{T} with relative and absolute tolerances ε_r and ε_a respectively.

```

1 function  $H = \text{HSSCompress}(A, \mathcal{T})$ 
2    $R \leftarrow \text{randn}(\text{rows}(A), d_0)$ 
3    $\text{CompressNode}(A, R, AR, A^*R, \text{root}(\mathcal{T}))$ 
4   return  $\mathcal{T}$ 

5 function  $\text{CompressNode}(A, R, S^r, S^c, \tau)$ 
6   if  $\text{isleaf}(\tau)$  then
7      $\tau.D \leftarrow A(\tau.I, \tau.I)$ 
8   else
9      $\nu_1, \nu_2 \leftarrow \text{children}(\tau)$ 
10     $\text{CompressNode}(A, R, S^r, S^c, \nu_1)$  // recursive compression ..
11     $\text{CompressNode}(A, R, S^r, S^c, \nu_2)$  // of child nodes
12     $\tau.B_{12} \leftarrow A(\nu_1.I^r, \nu_2.I^c)$ 
13     $\tau.B_{21} \leftarrow A(\nu_2.I^r, \nu_1.I^c)$ 
14  end
15  if  $\text{isroot}(\tau)$  then return
16   $\text{ComputeLocalSamples}(R, S^r, S^c, \tau, 1 : \text{cols}(R))$ 
17   $\{(\tau.U)^*, \tau.J^r\} \leftarrow \text{ID}((\tau.S^r)^*, \varepsilon_r/\text{level}(\tau), \varepsilon_a/\text{level}(\tau))$ 
18   $\{(\tau.V)^*, \tau.J^c\} \leftarrow \text{ID}((\tau.S^c)^*, \varepsilon_r/\text{level}(\tau), \varepsilon_a/\text{level}(\tau))$ 
19   $\text{ReduceLocalSamples}(R, \tau, 1 : \text{cols}(R))$ 

```

Algorithm 2: Compute local samples and reduce local samples based on rows selected by the interpolative decomposition.

```

1 function  $\text{ComputeLocalSamples}(R, S^r, S^c, \tau, i)$ 
2   if  $\text{isleaf}(\tau)$  then
3      $\tau.S^r(:, i) \leftarrow S^r(\tau.I, i) - \tau.D R(\tau.I, i)$ 
4      $\tau.S^c(:, i) \leftarrow S^c(\tau.I, i) - (\tau.D)^* R(\tau.I, i)$ 
5   else
6      $\nu_1, \nu_2 \leftarrow \text{children}(\tau)$ 
7      $\tau.S^r(:, i) \leftarrow \begin{bmatrix} \nu_1.S^r(\nu_1.J^r, i) - \tau.B_{12} \nu_2.R^r \\ \nu_2.S^r(\nu_2.J^r, i) - \tau.B_{21} \nu_1.R^r \end{bmatrix}$ 
8      $\tau.S^c(:, i) \leftarrow \begin{bmatrix} \nu_1.S^c(\nu_1.J^c, i) - (\tau.B_{21})^* \nu_2.R^c \\ \nu_2.S^c(\nu_2.J^c, i) - (\tau.B_{12})^* \nu_1.R^c \end{bmatrix}$ 
9   end

10 function  $\text{ReduceLocalSamples}(R, \tau, i)$ 
11  if  $\text{isleaf}(\tau)$  then
12     $\tau.R^r \leftarrow (\tau.V)^* R(\tau.I, i)$ ;  $\tau.I^c \leftarrow \tau.I(\tau.J^c)$ 
13     $\tau.R^c \leftarrow (\tau.U)^* R(\tau.I, i)$ ;  $\tau.I^r \leftarrow \tau.I(\tau.J^r)$ 
14  else
15     $\nu_1, \nu_2 \leftarrow \text{children}(\tau)$ 
16     $\tau.R^r \leftarrow (\tau.V)^* \begin{bmatrix} \nu_1.R^r \\ \nu_2.R^r \end{bmatrix}$ ;  $\tau.I^r \leftarrow [\nu_1.I^r \ \nu_2.I^r] (\tau.J^r)$ 
17     $\tau.R^c \leftarrow (\tau.U)^* \begin{bmatrix} \nu_1.R^c \\ \nu_2.R^c \end{bmatrix}$ ;  $\tau.I^c \leftarrow [\nu_1.I^c \ \nu_2.I^c] (\tau.J^c)$ 
18  end

```

<code>randn(m, n)</code>	an $m \times n$ matrix with iid $\mathcal{N}(0, 1)$ elements
<code>rows(A)/cols(A)</code>	number of rows/columns in matrix A
<code>isleaf(τ)</code>	true if τ is a leaf node, false otherwise
<code>isroot(τ)</code>	true if τ is a root node, false otherwise
<code>children(τ)</code>	a list with the children of node τ , always zero or two
<code>levels(\mathcal{T})</code>	number of levels in tree \mathcal{T}
<code>level(τ)</code>	level of node τ , starting from 0 at the root
<code>$\{Q, r\} \leftarrow \text{RRQR}(S, \varepsilon_r, \varepsilon_a)$</code>	rank-revealing QR, orthonormal Q and rank r

TABLE 1

List of helper functions.

traversal, calling the helper functions `ComputeLocalSamples` (computation of $\tau.S^r$ and $\tau.S^c$, Eqs. (2.5) and (2.13)) and `ReduceLocalSamples` (computation of $\tau.R^r$ and $\tau.R^c$) which are defined in Algorithm 2. After successful HSS compression, each non-leaf HSS node τ stores $\tau.B_{\nu_1, \nu_2}$, and each non-leaf node stores $\tau.U$ and $\tau.V$, although in practice, $\tau.U$ is stored using $\tau.\Pi^r$ and $\tau.E^r$.

In [14], we have extended the randomized HSS construction algorithm to make it adaptive, relaxing the condition that the maximum HSS is known *a priori*. This adaptive scheme is illustrated in Algorithm 3 and it works as follows. Each HSS node has a state field which can be `UNTOUCHED`, `COMPRESSED` or `PARTIALLY_COMPRESSED`. Each node starts in the `UNTOUCHED` state. The compression proceeds bottom-up from the leaf nodes, as in the non-adaptive Algorithm 1, with an initial number of random vectors d_0 . At each (non-root) node τ , bases U_τ and V_τ are computed using the ID, which, however, might fail if it is detected that random projection with d_0 random vectors is not sufficient to accurately capture the range of the corresponding Hankel block with a prescribed relative or absolute tolerance ε_{rel} or ε_{abs} respectively. How this can be detected will be discussed in detail in the following sub-sections. If at a node in the HSS tree, it is decided that d_0 is not sufficient, that node is marked as `PARTIALLY_COMPRESSED` and the compression algorithm returns to the outer loop. Note that in a parallel run, processing of other HSS nodes in independent sub-trees can still continue. The number of random projection vectors is increased by Δd and the recursive HSS compression is called again. At this point, there will be at least one node in the HSS tree which is in the `PARTIALLY_COMPRESSED` state. All of the descendants of this node are in the `COMPRESSED` state (or compression of that `PARTIALLY_COMPRESSED` could not have been started), and all of the ancestors are in the `UNTOUCHED` state. The compression algorithm will again start at the leaf nodes. For the already `COMPRESSED` nodes, the U and V bases do not need to be recomputed, but these nodes still need to be visited in order to add Δd extra columns to $\tau.S^r/\tau.S^c$ (Eqs. (2.5) and (2.13)) and $\tau.R^r/\tau.R^c$. For a graphical representation of the adaptive compression procedure see Figure 3.

Algorithm 3: Adaptive HSS compression of $A \in \mathbb{R}^{N \times N}$ using cluster tree \mathcal{T} with relative and absolute tolerances ε_r and ε_a respectively.

```

1 function  $H = \text{HSSCompressAdaptive}(A, \mathcal{T})$ 
2    $d \leftarrow d_0$ ;  $\Delta d \leftarrow 0$ ;  $R \leftarrow \text{randn}(N, d)$ ;  $S^r \leftarrow AR$ ;  $S^c \leftarrow A^*R$ 
3   foreach  $\tau \in \mathcal{T}$  do  $\tau.\text{state} \leftarrow \text{UNTOUCHED}$ 
4   while  $\text{root}(\mathcal{T}).\text{state} \neq \text{COMPRESSED}$  and  $d < d_{\max}$  do
5      $\text{CompressNodeAdaptive}(A, R, S^r, S^c, \text{root}(\mathcal{T}), \varepsilon, d, \Delta d)$ 
6      $\Delta d \leftarrow d$  or  $c^{st}$  // double or increment?
7      $\bar{R} \leftarrow \text{randn}(N, \Delta d)$ ;  $R \leftarrow [R \ \bar{R}]$ 
8      $S^r \leftarrow [S^r \ A\bar{R}]$ ;  $S^c \leftarrow [S^r \ A^*\bar{R}]$ 
9      $d \leftarrow d + \Delta d$ 
10  end
11  return  $\mathcal{T}$ 

12 function  $\text{CompressNodeAdaptive}(A, R, S^r, S^c, \tau, d, \Delta d)$ 
13  if  $\text{isleaf}(\tau)$  then
14    if  $\tau.\text{state} = \text{UNTOUCHED}$  then  $\tau.D \leftarrow A(\tau.I, \tau.I)$ 
15  else
16     $\nu_1, \nu_2 \leftarrow \text{children}(\tau)$ 
17     $\text{CompressNodeAdaptive}(A, R, S^r, S^c, \nu_1, d, \Delta d)$ 
18     $\text{CompressNodeAdaptive}(A, R, S^r, S^c, \nu_2, d, \Delta d)$ 
19    if  $\nu_1.\text{state} \neq \text{COMPRESSED}$  or  $\nu_2.\text{state} \neq \text{COMPRESSED}$  then return
20    if  $\tau.\text{state} = \text{UNTOUCHED}$  then
21       $\tau.B_{12} \leftarrow A(\nu_1.I^r, \nu_2.I^c)$ ;  $\tau.B_{21} \leftarrow A(\nu_2.I^r, \nu_1.I^c)$ 
22  end
23  if  $\text{isroot}(\tau)$  then  $\tau.\text{state} \leftarrow \text{COMPRESSED}$ ; return
24  if  $\tau.\text{state} = \text{UNTOUCHED}$  then
25     $\text{ComputeLocalSamples}(R, S^r, S^c, \tau, 1 : d + \Delta d)$ 
26  else  $\text{ComputeLocalSamples}(R, S^r, S^c, \tau, d + 1 : d + \Delta d)$ 
27  if  $\tau.\text{state} \neq \text{COMPRESSED}$  then
28    try
29       $\{(\tau.U)^*, \tau.J^r\} \leftarrow \text{ID}((\tau.S^r)^*, \varepsilon_r/\text{level}(\tau), \varepsilon_a/\text{level}(\tau))$ 
30       $\{(\tau.V)^*, \tau.J^c\} \leftarrow \text{ID}((\tau.S^c)^*, \varepsilon_r/\text{level}(\tau), \varepsilon_a/\text{level}(\tau))$ 
31       $\tau.\text{state} \leftarrow \text{COMPRESSED}$ 
32       $\text{ReduceLocalSamples}(R, \tau, 1 : d + \Delta d)$ 
33    catch // RRQR/ID failed to reach tolerance  $\varepsilon_r$  or  $\varepsilon_a$ 
34       $\tau.\text{state} \leftarrow \text{PARTIALLY\_COMPRESSED}$ 
35      return
36  else  $\text{ReduceLocalSamples}(R, \tau, d + 1 : d + \Delta d)$ 

```

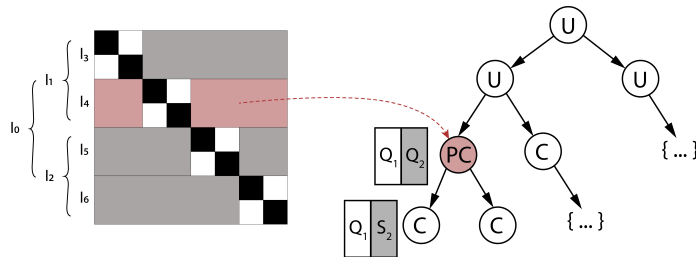


FIG. 3. Illustration of the tree traversal during adaptive HSS compression. Each node in the tree can be in either UNTOUCHED (U), PARTIALLY_COMPRESSED (PC), or COMPRESSED (C) state. For the meaning of the Q and S matrices, see Section 2.4.2.

Theorem 4.2 in [17] shows that for a matrix A and its HSS approximation H , with a total of L levels, and with each off-diagonal block compressed with tolerance ε , it holds that $\|A - H\| \leq L\varepsilon$. Inspired by this result, in the HSS compression, Algorithms 1 and 3, the user requested absolute and relative tolerances ε_a and ε_r are scaled with the current HSS level for the rank-revealing QR factorization. Hence, it is expected that the final HSS compression satisfies $\|A - H\| \leq \varepsilon_a$ or $\|A - H\|/\|A\| \leq \varepsilon_r$.

2.3. Difficulties with Adaptive Sampling. In this section we discuss some difficulties associated with the adaptive randomized HSS construction algorithm as described in Section 2.2, Algorithm 3. The main issue is to decide whether the sample matrices S^r and S^c capture the column space of the corresponding Hankel blocks well enough. As we shall see later, this decision relies on a good estimate of the matrix norm and hence the error estimation of the residual matrix (see Eq. (2.20)). A good error estimation is critical in devising the stopping criteria of adaptation. The goal is to ensure sufficient samples are used to guarantee the desired accuracy is, while not to perform too much oversampling, as this degrades performance. We first review a well-known result from the literature, and explain how it falls short when used as a stopping criterion. Then in Section 12 we propose our new approach.

From [10], we have the following lemma:

LEMMA 2.1 (Lemma 4.1 in [10]). *Let B be a real $m \times n$ matrix. Fix a positive integer p and a real number $\alpha > 1$. Draw an independent family $\{\omega^i : i = 1, \dots, p\}$ of standard Gaussian vectors. Then*

$$(2.15) \quad \|B\|_2 \leq \alpha \sqrt{\frac{2}{\pi}} \max_{i=1, \dots, p} \|B\omega^i\|_2$$

except with probability α^{-p} .

We will refer to the parameter p as the oversampling parameter. The value of α can be used as a trade-off, making the bound less strict or less probable. Consider for instance $\alpha = 10$ and $p = 10$. Then the bound in (2.15) holds with very high probability 10^{-10} . In [11], relation (2.15) is used as a stopping criterion in an adaptive HSS construction algorithm, with $B = (I - QQ^*)F$, as

$$(2.16) \quad \|(I - QQ^*)F\|_2 \leq \alpha \sqrt{\frac{2}{\pi}} \max_{i=1, \dots, p} \|(I - QQ^*)F\omega^i\|_2 \leq \varepsilon$$

where F is a Hankel block of the input matrix A , Q is a matrix with orthonormal columns which approximates the range of F , and ε is tolerance. The column dimension of Q is increased until the second inequality in (2.16) is satisfied, which guarantees that $\|(I - QQ^*)F\|_2 \leq \varepsilon$. There are two drawbacks with this criterion: 1) Since (2.15) gives an upper bound, the error might be drastically overestimated; 2) if different F blocks vary greatly in size, then different blocks will be compressed to different *relative* tolerances, even though they are compressed to the same *absolute* tolerance.

The potential overestimation of the error is not the main difficulty. The error estimate in (2.16) assumes that we have access to the entire matrix Hankel block F and the associated random samples. However, in the randomized matrix-free HSS construction as described in Section 2.2, only the local random samples $\tau.S^r$ and $\tau.S^c$ are available. In (2.10)-(2.13), the random sample matrix S_τ^r of the Hankel block corresponding to HSS node τ , i.e., $A(I_\tau, I_A \setminus I_\tau)$, is expressed in terms of the basis generators U_{ν_1} and U_{ν_2} of its children, see Eq. (2.13). The random sample S_τ^r of

the Hankel block is constructed by subtracting the random sample $D_\tau R(I_\tau, \cdot)$ of the diagonal block, see (2.10), using the already compressed D_τ (D_τ is exact only at the leaves). Hence, this introduces an approximation error, see (2.12). Another issue arises due to the HSS nested basis property, see Eq. (2.3). In order to maintain the HSS nested basis property, the Hankel block is not compressed directly, but only its coefficient in the $[U_{\nu_1} \ 0; 0 \ U_{\nu_2}]$ basis is compressed. This coefficient is defined in (2.14) as $\tau \cdot S^\tau$. The difficulty arises from the use of the interpolative decomposition to compress the off-diagonal blocks, see (2.6), since it leads to non-orthonormal bases U_τ . Hence, the bound from Lemma 2.1 should really be applied to

$$(2.17) \quad \left\| \begin{bmatrix} U_{\nu_1} & 0 \\ 0 & U_{\nu_2} \end{bmatrix} (I - Q_\tau Q_\tau^*) S_\tau \right\|_2,$$

to derive a correct stopping criterion for adaptive HSS compression. As long as the U bases are orthonormal, there is no problem, since $\|\cdot\|_2$ is unitarily invariant. In practice, a (strong) rank-revealing QR factorization [7] will cause the U matrices to be well-conditioned, and its elements to be bounded [10], so the absolute tolerance should not be affected much. It seems plausible for the non-orthonormal factors to essentially cancel out when using the relative stopping criterion, making it a more reliable estimate. Due to the hierarchical nature of the U and V matrices, it would be possible to compute the matrix products in Eq. (2.17) if this would be desired.

The error bound in Lemma 2.1 is not conducive to relative error bounds because it only bounds the error, not the matrix norm. It is not possible to use this bound in an attempt to compute a relative stopping criterion. In Section 2.4.2, we propose a new stopping criterion for adaptive HSS compression based on both absolute and relative bounds, inspired by Lemma 2.1, and the derivation of the accurate relative bound is given in Section 2.5.

2.4. Adaptive Sampling Strategies. While traversing the HSS tree during compression, a node may fail to compress to the desired accuracy due to a lack of random samples; this node, which corresponds to one off-diagonal Hankel block of the matrix A , is then labeled as `PARTIALLY_COMPRESSED`. We consider two strategies to add more random vectors: `DOUBLING`, and `INCREMENTING`. There are advantages and disadvantages to both approaches. Algorithms 4 (`DOUBLING`) and 5 (`INCREMENTING`) present the two strategies for the computation of an approximate basis for the range of a matrix A . Algorithms 4 and 5 correspond to the successive (rank-revealing) QR factorizations at the `PARTIALLY_COMPRESSED` node, and is part of the bigger Algorithm 3. The successive random sampling steps are actually performed in Algorithms 3, but are included here for convenience. In this section, Algorithms 4 and 5 are presented as only returning the orthonormal basis of the range of A , but when used in the overall HSS compression, Algorithm 3, also the upper triangular factor from the final rank-revealing QR factorization is required.

2.4.1. Doubling Strategy with Oversampling. Algorithm 4 computes an (orthogonal) approximate basis for the range of an $m \times n$ matrix A , with an oversampling parameter p , up to a given relative or absolute tolerance ε_r or ε_a . Initially, a random projection of the input matrix A with a tall and skinny random matrix R , with $d_0 + p$ columns, is computed as $S = AR$. Let Q be an orthonormal basis for S . From [10, Theorem 1.1], we have

$$(2.18) \quad \mathbb{E}\|(I - QQ^*)A\| \leq \left[1 + 4 \frac{\sqrt{d_0 + p}}{p - 1} \cdot \sqrt{\min\{m, n\}} \right] \sigma_{d_0+1}.$$

Algorithm 4: Adaptive computation of Q , an approximate basis for the range of the Hankel block A , using the DOUBLING strategy with an oversampling parameter p .

```

1 function  $Q = \text{RS-DOUBLING}(A, d_0, p, \varepsilon_r, \varepsilon_a)$ 
2    $k \leftarrow 1$ ;  $m \leftarrow \text{rows}(A)$ ;  $r \leftarrow \infty$ 
3    $R_1 \leftarrow \text{randn}(m, d_0 + p)$ 
4    $S_1 \leftarrow AR_1$ 
5   while ( $r > 2^{k-1}d_0$ ) do
6      $\{Q, r\} \leftarrow \text{RRQR\_HMT}(S_k, \varepsilon_r, \varepsilon_a)$ 
7      $\Delta d \leftarrow 2^{k-1}d_0 + p$  // double sample size
8      $R_{k+1} \leftarrow \text{randn}(m, \Delta d)$ 
9      $S_{k+1} \leftarrow [S_k \ AR_{k+1}]$ 
10     $k \leftarrow k + 1$ 
11  end
12  return  $Q$ 

```

where σ_{d_0+1} is the (d_0+1) -th singular value of A . The factor in brackets in Eq. (2.18), the deviation from the optimal error σ_{d_0+1} , decreases with increasing oversampling p . In order to guarantee a relative or absolute error bound on $\|A - QQ^*A\|$, we apply a modified RRQR factorization (a column pivoted QR) to S , which includes this factor. The modified RRQR (`RRQR_HMT` in Algorithm 4) return a rank $r = k$ as soon as

(2.19)

$$R_{k,k} \leq \frac{\varepsilon_a}{1 + 4 \frac{\sqrt{d_0+p}}{d_0+p-k-1} \cdot \sqrt{\min\{m, n\}}} \quad \text{or} \quad \frac{R_{k,k}}{R_{1,1}} \leq \frac{\varepsilon_r}{1 + 4 \frac{\sqrt{d_0+p}}{d_0+p-k-1} \cdot \sqrt{\min\{m, n\}}}.$$

This modification is to take into account that at step k of the `RRQR_HMT` algorithm, the amount of oversampling is $d_0 + p - k - 1$. If the rank r returned by the modified RRQR is $r < d_0$, i.e., at least p oversampling vectors are used, then the orthonormal basis Q returned by RRQR is accepted. However, if RRQR does not achieve the required tolerance, or if it achieves the required tolerance but $d_0 \leq r \leq d_0 + p$, then the resulting Q basis is rejected. The number of random vectors (excluding the p oversampling columns) is doubled and the random projection with these new vectors is added to S . A rank-revealing QR factorization is applied to the entire new random projection matrix S . Since in this scenario RRQR is always redone from scratch, the number of adaptation steps should be minimized in order to minimize the work in RRQR. Doubling the number of random vectors in each step ensures one only needs $\mathcal{O}(\log(r))$ adaptation steps¹, but in the worst-case scenario, the amount of oversampling is $r/2 - 1 + p$.

This is the approach used in [14, 6, 5] for adaptive randomized HSS construction, although in these references, the scaling factor from Eq. (2.18) was not included. Including this scaling factor slightly increases the rank, but gives more accurate compression. When used in the larger HSS compression algorithm, the matrix sizes m and n from Eq. (2.19) are the sizes of the original Hankel block.

2.4.2. Incrementing Strategy based on Lemma 2.1. Algorithm 5 presents a new approach to adaptive rank determination. The adaptive scheme used in Algorithm 4 performs a rank-revealing factorization in each adaptation step with a

¹Logarithm is in base 2 throughout the paper.

Algorithm 5: Adaptive computation of Q , an approximate basis for the range of the Hankel block A , using the INCREMENTING strategy.

```

1 function  $Q = \text{RS-INCREMENTING}(A, d_0, \Delta d, \varepsilon_r, \varepsilon_a)$ 
2    $k \leftarrow 1$ ;  $m \leftarrow \text{rows}(A)$ ;  $Q \leftarrow []$ 
3    $R_1 \leftarrow \text{randn}(m, d_0)$ 
4   while true do
5      $S_k \leftarrow AR_k$  // new samples
6      $\hat{S}_k \leftarrow (I - QQ^*)^2 S_k$  // iterated block Gram-Schmidt
7     if ( $\|\hat{S}_k\|_F / \|S_k\|_F < \varepsilon_r$  or  $\|\hat{S}_k\|_F / \sqrt{\Delta d} < \varepsilon_a$ ) then break
8      $\{Q_k, \bar{R}_k\} \leftarrow \text{QR}(\hat{S}_k)$ 
9     if  $\min(\text{diag}(|\bar{R}_k|)) < \varepsilon_a$  or  $\min(\text{diag}(|\bar{R}_k|)) < \varepsilon_r |(\bar{R}_1)_{11}|$  then
10      break
11      $Q \leftarrow [Q \ Q_k]$ 
12      $k \leftarrow k + 1$ 
13      $R_k \leftarrow \text{randn}(m, \Delta d)$ 
14 end
15  $\{Q, r\} \leftarrow \text{RRQR}([S_1 \ \dots \ S_k], \varepsilon_r, \varepsilon_a)$ 
16 return  $Q$ 

```

random projection matrix that is double the size of that in the previous step. The rank-revealing factorization has to be performed from scratch in each step, which leads to additional computational cost and communication. In particular, the communication involved in column pivoting in the repeated RRQR factorizations can be a serious bottleneck in a distributed memory code. In contrast, in Algorithm 5, the rank-revealing factorization is only performed when the number of sample vectors is guaranteed to be sufficient. This decision criterion is based on relation (2.16) and uses an adaptive blocked implementation.

In [10], Algorithm 4.2 (“Adaptive Randomized Range Finder”) is presented for the adaptive computation of an orthonormal basis Q for the range of a matrix A , up to an absolute tolerance ε_a . This algorithm computes an approximate orthonormal basis for the range of A one vector at a time and then determines how well this basis approximates the range. Adding one vector at a time to the basis amounts to performing multiple matrix-vector products (BLAS-2), which are memory-bound and less efficient on modern hardware. In [11], Algorithm 2 (“Parallel adaptive randomized orthogonalization”) uses an approach similar to Algorithm 4.2 in [10], but implements a blocked version, relying on BLAS-3 operations which can achieve much higher performance. This also relies on an absolute tolerance only. Algorithm 5 implements a blocked version, but it uses both an absolute and a relative stopping criterion. The stopping criterion is based on a stochastic error bound and block Gram-Schmidt orthogonalization [15, 13].

Let Q be an orthonormal approximate basis for the range of an $m \times n$ matrix A . Given a random Gaussian matrix $R \in \mathbb{R}^{n \times d}$, compute first the random samples $S = AR$ followed by the projection $\hat{S} = (I - QQ^*)S$. This last operation is a step of block Gram-Schmidt. In practice, to ensure orthogonality, we apply this step twice [15]. Thus, \hat{S} contains information about the range of A that is not included in Q . A small $\|\hat{S}\|_F$ means that either Q was already a good basis for the range of A , or S was in the range of Q , which is unlikely. If $\|\hat{S}\|_F$ is not small enough, \hat{S} is used

to expand Q . Since \widehat{S} is already orthogonal to Q , \widehat{S} only needs to be orthogonalized using a QR factorization, $[\widehat{Q}, R] = \text{QR}(\widehat{S})$, and can then be added to $Q \leftarrow [Q \ \widehat{Q}]$.

Additional difficulties arise in the blocked version that do not appear in the single vector case. Adding single vectors to the basis always ensures that each basis vector adds new information. In the blocked case however, \widehat{S} can become (numerically) rank-deficient. Therefore, in Algorithm 5, Line 9, we look at the diagonal elements of \overline{R} in order to determine if \widehat{S} is rank-deficient. If the diagonal elements of \overline{R} are less than a specified tolerance (relative or absolute), then we have complete knowledge of the range space (up to the specified tolerance) and we can compress the HSS node.

A similar approach is used in [11] with an absolute tolerance, based on Lemma 2.1. We have been unable to find an explicit reference to a *relative* stopping criterion. From [18, 19] we know that using a relative tolerance for the compression of off-diagonal blocks leads to a relative error in the Frobenius norm. Since this is frequently desired, our Algorithm 5 uses both absolute and relative stopping criteria explicitly. Relative tolerances are especially useful if the magnitude of different matrix sub-blocks differ significantly. By continuing the example above, we will compute the interpolative decomposition at a node if either condition is satisfied:

$$(2.20) \quad \frac{\min_i |\overline{R}_{ii}|}{\rho} < \varepsilon_r, \quad \min_i |\overline{R}_{ii}| < \varepsilon_a, \quad \frac{\|\widehat{S}\|_F}{\|S\|_F} < \varepsilon_r, \quad \frac{1}{\sqrt{d}} \|\widehat{S}\|_F < \varepsilon_a.$$

Here, ρ characterizes the largest value in the \overline{R} matrices. A few possible choices are $|(\overline{R}_1)_{11}|$, $\max_j |(\overline{R}_1)_{jj}|$, or $\max_{k,j} |(\overline{R}_k)_{jj}|$. As soon as one of the above stopping criteria is satisfied, a rank-revealing factorization is applied to all of the computed random samples.

Ideally, we would like to bound our errors with respect to A : $\|(I - QQ^*)A\|_F / \|A\|_F$ and $\|(I - QQ^*)A\|_F$, where A is a Hankel block of the original input matrix. However, since A might not be readily available (or expensive to compute), we instead use the random samples S . In the next section we establish a stochastic F -norm relationship between $\|A\|_F$ and $\|S\|_F$ and, in Appendix A, show that this estimate is accurate to high probability.

2.5. Mathematical Theory. We now present the probability theory for the stopping criterion described by Eq. (2.20), and used in Algorithm 5. Let $A \in \mathbb{R}^{m \times n}$ and $x \in \mathbb{R}^n$ with $x_i \sim \mathcal{N}(0, 1)$. Let

$$(2.21) \quad A = U\Sigma V^* = \begin{bmatrix} U_1 & U_2 \end{bmatrix} \begin{bmatrix} \Sigma_r & 0 \\ 0 & 0 \end{bmatrix} \begin{bmatrix} V_1^* \\ V_2^* \end{bmatrix}$$

be the singular value decomposition (SVD) of A , and let $\xi = V^*x$. Since x is a Gaussian random vector, so is ξ . By the rotational invariance of $\|\cdot\|_2$, it follows that

$$(2.22) \quad \|Ax\|_2^2 = \|\Sigma\xi\|_2^2 = \sigma_1^2 \xi_1^2 + \cdots + \sigma_r^2 \xi_r^2,$$

with $\sigma_1 \geq \cdots \geq \sigma_r > 0$ the positive singular values. Hence,

$$(2.23) \quad \mathbb{E} \left(\|Ax\|_2^2 \right) = \sigma_1^2 + \cdots + \sigma_r^2 = \|A\|_F^2.$$

In order to facilitate analysis, we define

$$(2.24) \quad X \sim \sigma_1^2 \xi_1^2 + \cdots + \sigma_r^2 \xi_r^2,$$

where $\xi_i \sim \mathcal{N}(0, 1)$, and thus $\mathbb{E}(X) = \|A\|_F^2$. From (2.22), we see that $\|Ax\|_2^2$ and X have the same probability distribution, so we focus on understanding X . Consider

$$(2.25) \quad \bar{X}_d \sim \frac{1}{d}(X_1 + \cdots + X_d),$$

where X_i are independent realizations of X . It is easy to see that $\mathbb{E}(\bar{X}_d) = \|A\|_F^2$. Using Chernoff's inequality [2], we prove the following theorem, stating that the probability tails of X and \bar{X}_d decay exponentially away from $\|A\|_F^2$.

THEOREM 2.2 (Probabilistic Error Bounds). *Given \bar{X}_d as defined in Eq. (2.25), the following bounds on the tail probabilities hold:*

$$(2.26) \quad \begin{aligned} \mathbb{P}\left[\bar{X}_d \geq \|A\|_F^2 \tau\right] &\leq \exp\left(-\frac{d\tau}{2}\right) \|A\|_F^{dr} \prod_{k=1}^r (A'_k)^{-d} & \tau > 1 \\ \mathbb{P}\left[\bar{X}_d \leq \|A\|_F^2 \tau\right] &\leq \exp\left(-\frac{d\tau}{2}\right) \|A\|_F^{dr} \prod_{k=1}^r (A''_k)^{-d} & \tau \in [0, 1). \end{aligned}$$

Here, $\|A\|_F^2 = \sigma_1^2 + \cdots + \sigma_r^2$, $(A'_k)^2 = \|A\|_F^2 - \sigma_k^2$, and $(A''_k)^2 = \|A\|_F^2 + \sigma_k^2$. We know that $\mathbb{E}(\bar{X}_d) = \|A\|_F^2$, so τ controls multiplicative deviation above or below the expectation value.

The proof is relegated to Appendix A. From Theorem 2.2, we see that if $R \in \mathbb{R}^{n \times d}$ with $R_{jk} \sim \mathcal{N}(0, 1)$, it is clear that

$$(2.27) \quad \frac{1}{\sqrt{d}} \sqrt{\mathbb{E}(\|AR\|_F^2)} = \|A\|_F,$$

and particular realizations will, with high probability, be close to the expected value. Hence, Theorem 2.2 shows that the matrix Frobenius norm can be accurately predicted using just (Gaussian) random samples of the range. In particular, we can approximate the difference between our approximation and the actual matrix sub-block, allowing us to compute both the absolute and relative error in contrast to Lemma 2.1. Future work investigating a random variable whose expectation value is $\|A\|_2$ (or some power) would be beneficial. At this point, we settle for using the Frobenius norm because we can accurately approximate it.

2.6. Flop Counts: Doubling vs. Incrementing. First, note that the full QR factorization $Q = \text{QR}(A)$ for $A \in \mathbb{R}^{m \times n}$ (with $m \gg n$) performs $2mn^2$ floating point operations (flops). Assuming the numerical rank of A is r , then the rank-revealing QR factorization $Q = \text{RRQR}(A)$ requires $2mnr$ flops. Given $S \in \mathbb{R}^{m \times r}$ and $X \in \mathbb{R}^{m \times d}$, the orthogonalization $S \leftarrow (I - XX^*)S$ requires $4mdr$ flops (ignoring a lower order mr term), and twice that for the iterated ($2 \times$) block Gram-Schmidt step.

In the DOUBLING strategy, Algorithm 4, at step k , $2^{k-1}d_0 + p$ random vectors have already been sampled, where p is a small oversampling parameter (e.g. $p = 10$). Then, $2^{k-1}d_0$ new random samples are added to the sample matrix S_k , leading to $2^k d_0 + p$ columns for S_k . Except for the final step, the operation $Q_k \leftarrow \text{RRQR}(S_k)$ costs $\sim 2m4^k d_0^2$ flops. In the final step, the RRQR terminates early when the tolerance is met at rank r , with a cost of $\sim 2mr^2$ flops. The total number of steps needed to reach the final rank r is $N \sim \log(r/d_0)$. Summing the costs of N steps: $2md_0^2 \sum_{k=1}^N 4^k$, we obtain the total flop count of $\sim \frac{8}{3}mr^2$.

The INCREMENTING strategy, Algorithm 5, starts with d_0 random samples and adds Δd new random vectors at each step. At step k we have the sample matrix $S = [S_1 \cdots S_k]$, and the orthogonal matrix $Q = [Q_1 \cdots Q_{k-1}]$. We first compute the orthogonal projection $\hat{S}_k \leftarrow (I - QQ^*)^2 S_k$, which costs $8m(k-1)\Delta d^2$ flops, followed by $Q_k \leftarrow \text{QR}(\hat{S}_k)$, which costs $2m\Delta d^2$, and then append Q_k to Q . The total number of steps needed to reach the final rank r is $N \sim (r - d_0)/\Delta d \sim r/\Delta d$. Summing the cost of N steps: $8m\Delta d^2 \sum_{k=1}^N (k-1)$, gives the overall cost $\sim 4mr^2$. The cost of the final RRQR is an additional $2mr^2$ flops.

From the above analysis, we see that the INCREMENTING scheme requires more flops. However, DOUBLING involves a larger amount of data movement due to the column pivoting needed in each step of RRQR. This manifests itself in the communication cost of the parallel algorithm, which will be analyzed in Section 3.3.

3. Parallel Algorithm. The parallel algorithm uses the same parallelization framework as described in [14, Section 3]. The data partitioning and layout is based on the HSS tree, following a proportional mapping of subtrees to subsets of processes in a top-down traversal. The HSS tree can be specified by the user. The tree should be binary, but can be imbalanced and does not need to be complete. For HSS nodes that are mapped to multiple processors, the matrices stored at those nodes are distributed in 2D block-cyclic (ScaLAPACK style) layout.

3.1. Partially Matrix-Free Interface. The randomized HSS compression algorithm is so-called “partially” matrix-free. This means it does not require every single element of the input matrix A . What is required is a routine to perform the random sampling $S = AR$, as well as a way to extract sub-blocks from A . Recall from Section 2.2 that at the leafs, $D_\tau = A(I_\tau, I_\tau)$. Furthermore, due to the use of interpolative decompositions, $B_{\nu_1, \nu_2} = A(J_{\nu_1}^r, J_{\nu_2}^c)$, is a sub-block of A .

If the input matrix A is given as an explicit dense matrix, the random sampling $S = AR$ is performed in parallel using the PBLAS routine PDGEMM with a 2D block-cyclic data layout for A , S and R . In this case, the input matrix A is also redistributed – with a single collective MPI call – from the 2D block-cyclic layout to a layout corresponding to the HSS tree, such that extraction of sub-blocks for D_τ and B_{ν_1, ν_2} does not require communication between otherwise independent HSS subtrees.

Instead of forming an explicit dense matrix A , the user can also specify multiplication and element extraction routines. The multiplication routine computes, for a given random matrix R , the random sample matrices $S^r = AR$ and $S^c = A^*R$. This is the more interesting use case, since for certain classes of structured matrices a fast multiplication algorithm is available; consider for instance sparse matrices, low-rank and hierarchical matrices, combinations of sparse and low-rank matrices or operators which can be applied using the fast Fourier transform or similar techniques. The element extraction routine should be able to return matrix sub-blocks $A(I, J)$, defined by row and column index sets I and J respectively. Depending on how the user data is distributed, computing matrix elements might involve communication between all processes. In this case, the HSS compression traverses the tree level by level (from the leafs to the root), with synchronization at each level and element extraction for all blocks D_τ and B_{ν_1, ν_2} on the same performed simultaneously in order to aggregate communication messages and minimize communication latency. If no communication is required for element extraction, then independent subtrees can be compressed concurrently.

3.2. Parallel Restart. During factorization, nodes can be in either UNTOUCHED (U), PARTIALLY_COMPRESSED (PC) or COMPRESSED (C) state. A node can not start compression until both it’s children are in the C state. If during HSS compression, a process encounters an internal HSS node which children that are not both in the C state, this process stops the HSS tree traversal. Independent subtrees can progress the compression further if they can compressed successfully with the current number of random samples. This can lead to load imbalances if the HSS tree, or the off-diagonal block ranks, are imbalanced. Eventually, all processes synchronize to perform the random sampling in parallel. Hence there is some overhead associated with restarting the HSS compression algorithm to add more random samples. In addition, random sampling is more efficient, in terms of floating point throughput, when performed with more random vectors at once.

3.3. Communication Cost in Parallel Adaptation. In [14], we analyzed the communication cost of the entire parallel HSS algorithm, assuming no adaptivity. In this section, we will focus only on the cost of adaptivity, using either DOUBLING or INCREMENTING strategy.

Consider the current node of the HSS tree that requires adaptation (called “PC” node). Assume the final rank is r , the row dimension of the sample matrix is m , and P processes work on this node in parallel. We use the pair [#messages, volume] to denote the *communication cost* which counts the number of messages and the number of words transferred for a given operation, typically along the critical path. A broadcast of W words among P processes has the cost $[\log P, W \log P]$. This assumes that broadcast follows a tree-based implementation: there are $\log P$ steps on the critical path (any branch of the tree) and W words are transferred at each step, yielding $\log P$ messages and $w \log P$ words.

For a rectangular matrix of dimension $m \times n$, assuming $m/P \geq n$, the communication cost for non-pivoted QR factorization (PDGEQRF in ScaLAPACK) is $[2n \log P, \frac{mn}{\sqrt{P}} \log P]$ [1, 4]. For QR factorization with column pivoting, i.e., PDGEQPF in ScaLAPACK, additional communication is needed at each step to compute the column norm and permutes the column with the maximum norm to the leading position. Computing the maximum column norm needs two reductions along row and column dimensions, costing $2 \log \sqrt{P} = \log P$ messages. The additional communication volume is of lower order term. In total, PDGEQPF has communication cost $[3n \log P, \frac{mn}{\sqrt{P}} \log P]$

In the DOUBLING strategy (Algorithm 4), we need $s = \log \frac{r}{d_0}$ steps of augmentations to reach the final rank r . At the k -th step, we perform RRQR (ID) for S_k of dimension $m \times d_0 2^k$, using PDGEQPF. The total communication cost of s steps sums up to:

$$(3.1) \quad \sum_{k=0}^s \left[3d_0 2^k \log P, \frac{m(d_0 2^k)}{\sqrt{P}} \log P \right] = \left[3d_0 \log P \sum_{k=0}^s 2^k, \frac{md_0}{\sqrt{P}} \log P \sum_{k=0}^s 2^k \right] \\ = \left[3d_0 2^{s+1} \log P, \frac{md_0 2^{s+1}}{\sqrt{P}} \log P \right] = \left[6r \log P, \frac{2mr}{\sqrt{P}} \log P \right].$$

In the INCREMENTING strategy (Algorithm 5), we need $s = \frac{r}{\Delta d}$ steps of increments to reach the final rank r . At the k -th step, two costly operations are the block Gram-Schmidt and block QR (Lines 6 and 8 respectively in Algorithm 5).

Each Gram-Schmidt orthogonalization step requires two matrix multiplications; we use PDGEMM in PBLAS, which uses a pipelined SUMMA algorithm [16]. The Q

matrix is of dimension $m \times d$, where $d = \Delta d(k-1)$. The S_k matrix is of dimension $m \times \Delta d$. The communication cost for $Q^* \cdot S_k$ is $[\Delta d, \frac{\Delta d(m+d)}{\sqrt{P}}]$. The cost for another multiplication $Q \cdot (Q^* \cdot S_k)$ is the same. Since we do Gram-Schmidt twice, the total communication cost of s steps sums up to:

$$(3.2) \quad 2 \cdot 2 \sum_{k=1}^s \left[\Delta d, \frac{\Delta d(m+d)}{\sqrt{P}} \right] = 4 \cdot \left[r, \sum_{k=1}^s \frac{m\Delta d + \Delta d^2 \cdot k}{\sqrt{P}} \right] = \left[4r, 4 \frac{mr + r^2/2}{\sqrt{P}} \right].$$

Next, we perform QR for \hat{S}_k of dimension $m \times \Delta d$, using PDGEQRF. The total communication cost of s steps sums up to:

$$(3.3) \quad \sum_{k=1}^s \left[2 \Delta d \log P, \frac{m \Delta d}{\sqrt{P}} \log P \right] = \left[2r \log P, \frac{mr}{\sqrt{P}} \log P \right].$$

Comparing Eqs. (3.2) and (3.3), we see that the communication in Gram-Schmidt is a lower order term compared to the QR factorizations, therefore we ignore it.

In a final step (Line 14 in Algorithm 5) we perform a large RRQR, with communication cost $[3r \log P, \frac{mr}{\sqrt{P}} \log P]$. This is added into Eq. (3.3). The leading cost of the INCREMENTING strategy is $[5r \log P, \frac{2mr}{\sqrt{P}} \log P]$. Compared to the DOUBLING strategy, the INCREMENTING strategy requires fewer messages, and has a similar communication volume.

4. Numerical Experiments.

4.1. Experiments Setup. Numerical experiments were conducted using the Cori supercomputer at NERSC. Each node has two sockets, each socket is populated with a 16-core Intel[®] Xeon[™] Processor E5-2698 v3 (“Haswell”) at 2.3 GHz and 128 GB of RAM memory. We used STRUMPACK v2.2 linked with Intel MKL and compiled with the Intel compilers version 17.0.1.132 in Release mode.

4.2. Test Problems. The first set of numerical experiments depicts six dense linear systems from a variety of applications in double precision (dp) and single-precision (sp). A complete description of the problems under consideration can be found on [14], with the exception of the first experiment at Table 2. The first experiment is the parameterized example $\alpha I + \beta UDV^*$. U and V are orthogonal matrices of rank r and are distributed in order to allow for fast element extraction and scalable tests, and D is either the identity matrix or a diagonal matrix with decaying entries, giving us a matrix that has off-diagonal blocks with either constant or decaying singular values. In this particular case we set $D_{k,k} = 2^{-53(k-1)/r}$, and $r = 500$. The largest experiments ($N = 500,000$) used $p = 1,024$ cores, whereas the rest of the experiments used $p = 64$ cores. Column three, HSS_ϵ , denotes the relative error of the HSS approximation, whereas the absolute error is kept constant at $1E-08$. Each experiment is performed at three increasingly tighter approximation tolerances, while we report on the three main stages involved in the solution of the linear system: Approximation–compression– of the dense matrix, factorization, and solve. The metrics of interest at each stage are memory consumption, flops, and max wall-clock time from all MPI ranks.

Numerical experiments (Table 2) show that compression takes the most flops and time, followed by factorization and solve, which are much cheaper in comparison.

Nonetheless, as we increase the accuracy of the approximation, we notice a moderate increase in the wall-clock time in all three stages.

TABLE 2
Solving linear systems from different applications.

Matrix	N	HSS $_{\epsilon}$	HSS compression				ULV* factorization			Solve	
			HSS rank	Mem (MB)	Flops $\times 10^{12}$	Time (s)	Mem (MB)	Flops $\times 10^{12}$	Time (s)	Flops $\times 10^9$	Time (s)
$\alpha I + \beta UDV^*$ (dp)	500k	1E-02	28	356	0.01	4.22	559	0.01	0.17	0.19	0.10
		1E-06	59	671	0.03	4.71	1343	0.03	0.18	0.45	0.14
		1E-10	73	868	0.06	4.93	1927	0.06	0.24	0.64	0.15
Toeplitz (dp)	500k	1E-02	2	40	0.70	1.50	64	0.001	0.11	0.02	0.06
		1E-06	2	40	0.70	1.52	64	0.001	0.11	0.02	0.08
		1E-10	2	40	0.70	1.62	64	0.001	0.11	0.02	0.09
Quantum Chem. (dp)	500k	1E-02	12	235	34.60	9.26	383	0.01	0.11	0.12	0.09
		1E-06	75	308	34.61	9.51	486	0.01	0.22	0.16	0.09
		1E-10	113	377	34.62	9.66	615	0.01	0.28	0.21	0.09
BEM Acoustic (dp)	10k	1E-02	723	363	2.49	6.10	770	0.40	0.91	0.54	0.09
		1E-06	1249	607	5.12	12.72	1304	1.12	1.91	0.91	0.17
		1E-10	1332	631	5.20	12.90	1366	1.23	1.97	0.95	0.27
BEM Sphere (sp)	27k	1E-01	500	159	9.77	11.16	364	0.13	0.55	0.47	0.09
		1E-03	1491	433	26.17	29.85	1089	1.20	1.91	1.39	0.16
		1E-05	2159	795	46.97	60.07	1908	3.57	4.63	2.51	0.20
Schur100 (sp)	10k	1E-01	287	42	1.00	1.98	93	0.02	0.33	0.12	0.09
		1E-03	412	81	1.20	2.60	193	0.08	0.43	0.26	0.08
		1E-05	471	111	1.77	3.67	257	0.14	0.44	0.34	0.04

4.3. Performance Breakdown. The second set of numerical experiments illustrates the new INCREMENTING adaptive technique in comparison with the traditional DOUBLING adaptive technique that relies on RRQR with column pivoting. Table 3 shows the detailed breakdown of the flops and time in different stages of the two algorithms for the BEM Sphere linear system with $d_0 = 128$ and $\Delta d = 256$, and using $p = 1,024$ cores.

The first observation is that in both INCREMENTING and DOUBLING, nearly 90% of the flops are in the initial sampling step. On the other hand, since the sampling step involves highly efficient matrix-matrix multiplication, the percentage time spent at this step is under 50%.

The second most costly step is ID, i.e., RRQR. It has less than 5% of the flops, but takes 28% and 37% time respectively. This shows that the data movement associated with column pivoting is expensive.

Using the same tolerance $1E - 3$, the INCREMENTING strategy achieves sufficient accuracy, while the DOUBLING strategy does more adaptations, leading to higher rank and the accuracy level more than needed, and taking longer time.

4.4. Adaptivity Performance.

4.4.1. Evaluation of New Stopping Criterion. This section considers the parametrized problem $\alpha I + \beta UDV^*$ with $N = 20,000$, $\alpha = 1$, $\beta = 1$ and $D_{k,k} = 2^{-53(k-1)/r}$, with $r = 200$, using $p = 256$ cores. We provide a comparison with the classical stopping criterion proposed in HMT [10], as shown in Table 4. In our strategy, we vary both relative (rtol) and absolute (atol) tolerance. HMT only works

TABLE 3

Performance breakdown. “Compute Samples” and “Reduce Samples” correspond to the two functions in Algorithm 2.

	Flops $\times 10^{12}$ (% Flops)		Time (% Time)	
	INCREMENTING	DOUBLING	INCREMENTING	DOUBLING
Compression	29.75	56.07	5.50	8.24
HSS Rank	1480	1945		
Relative error	2.40E-03	2.68E-04		
→ Random samp.	26.61 (89.5%)	50.22 (89.6%)	2.40 (43.5%)	3.93 (47.8%)
→ ID	0.85 (2.9%)	2.73 (4.9%)	1.54 (27.9%)	3.04 (36.9%)
→ QR	0.51 (1.7%)	-	0.52 (9.5%)	-
→ Orthogonalize	0.61 (2.1%)	-	0.18 (3.3%)	-
→ Comp. samples	1.08 (3.6%)	2.89 (5.2%)	0.55 (10.0%)	0.86 (10.4%)
→ Red. samples	0.09 (0.3%)	0.23 (0.4%)	0.32 (5.8%)	0.41 (5.0%)
Factorization	1.29	2.67	1.98	2.83
Solve	0.001	0.002	0.14	0.15

TABLE 4

New stopping criterion and HMT criterion [10]. Each entry has two numbers: one is the relative error of the HSS approximation given by $\|A - HSS * I\|_F / \|A\|_F$, another is the HSS rank.

		atol			
		1E-02	1E-06	1E-10	1E-14
rtol	1E-02	1.05E-02/43	1.05E-02/43	1.05E-02/43	1.05E-02/43
	1E-06	1.82E-05/77	1.82E-05/77	1.82E-05/77	1.82E-05/77
	1E-10	4.91E-06/87	5.18E-09/127	5.18E-09/127	5.18E-09/127
	1E-14	4.91E-06/87	6.68E-10/138	6.58E-13/187	6.58E-13/187
	HMT	3.14E-06/87	3.50E-10/139	3.61E-14/192	5.53E-15/5000+

with absolute tolerance, so we put it in the last row of the table.

It can be seen that with our new criterion, when we set “rtol” and “atol” to be the same, the approximation accuracy is at the same level of the requested tolerance (see the diagonal of Table 4).

With the HMT criterion, however, since it uses an upper bound as a termination metric, this in practice can be pessimistic, delivering an approximation error that is usually smaller than requested, at the expense of large ranks. From a user point of view it is difficult to choose a proper compression tolerance.

As a result, when the given tolerance is close to machine precision, HMT criterion requires many steps, as depicted in the bottom right corner of Table 4, where the algorithm terminated not due to achieving the “atol”, but because it reach the maximum allowable rank (5000 in this case). Thus, there will be some absolute tolerances which cannot be satisfied, yet it is not clear how small this tolerance is or how to determine it *before* attempting compression. Furthermore, it is not clear how to determine when this happens during compression, either. A relative tolerance is much easier to set and frequently of most practical interest.

4.4.2. Evaluation of Adaptivity Cost. In order to assess the cost associated with our adaptivity strategy, we performed the following experiments with two matrices for which we know the HSS ranks. Thus, we can choose a precise number of random vectors, so that there is no need for adaptation. This should be the fastest possible case, and we denote this as “known-rank”. Suppose we do not have adaptive strategy, the best a user can do is to restart compression from scratch (unable to reuse the partial compression results) when the final residual is large, manually increasing the number of random vectors. We denote this as “hard-restart”. In between these

TABLE 5

Evaluation of adaptivity cost. For all the tests, we use $atol = rtol = 1E - 14$, We use 1,024 cores for the first problem and 64 cores for the second one. With each strategy, we report the compression time (Compr. time), HSS rank, and the number of adaptation steps needed (# adapt.)

		“Known-rank”	INCREMENTING	“Hard-restart”
$I + UDV^*$ $d_0 = 128$ $\Delta d = 64$	Compr. time	36.5	37.2	100.3
	HSS-rank	1162	1267	1165
	Num. adapt.	0	17	4
$I + UDV^*$ $d_0 = 512$ $\Delta d = 128$	Compr. time	35.7	36.6	54.6
	HSS-rank	1162	1194	1161
	# adapt.	0	5	2
BEM Acoustics $d_0 = 128$ $\Delta d = 64$	Compr. time	11.15	12.5	18.3
	HSS-rank	1264	1334	1348
	# Adapt.	0	24	4
BEM Sphere $d_0 = 512$ $\Delta d = 128$	Compr. time	11.9	10.5	18.9
	HSS-rank	1276	1352	1362
	# Adapt.	0	9	2

two modes is our adaptive strategy INCREMENTING.

The first matrix is $I + UDV^*$, where $D_{k,k} = 2^{-53(k-1)/r}$, $r = 1200$, $N = 60,000$. The second matrix is the BEM Acoustic problem, with $N = 10,000$. Table 5 shows the compression times with different configurations of d_0 and Δd . It is clear that our adaptive strategy is nearly as fast as the fastest “known-rank” case, and is up to 2.7x faster than the “hard-restart”.

4.5. Scalability. The last numerical experiment depicts two strong scaling studies, as shown in Figure 4. The first test problem depicts the Quantum Chemistry dense linear system of size $N = 300,000$ and HSS relative approximation error of $1E - 2$ and HSS leaf size of 128. This matrix is amenable to efficient rank compression, resulting in an HSS rank of 12. In contrast, for a problem with larger numerical rank and tighter numerical accuracy, we show the scalability from the parametrized test case $\alpha I + \beta UDV^*$ with $N = 500,000$, $\alpha = 1$, $\beta = 1$ and $D_{k,k} = 2^{-53(k-1)/r}$, with $r = 500$. The resulting HSS rank is $r = 480$ at an HSS relative approximation tolerance of $1E - 14$ with HSS leaf size of 128. The first example scales better since its HSS rank is small and there is no need for adaptation, whereas the second example requires a few steps for rank adaptation, given that its HSS rank is quite large.

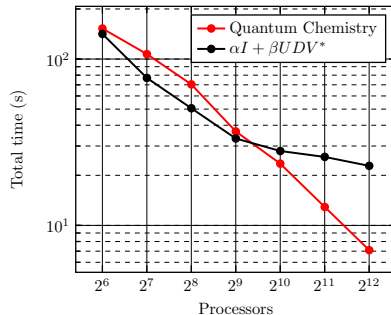


FIG. 4. Strong scaling experiment up to $p = 4,096$ cores of the Cori supercomputer. The Quantum Chemistry problem has $N = 300,000$ and HSS rank of 12, and the parametrized problem has $N = 500,000$ and HSS rank of 480.

5. Conclusion. We presented two new stopping criteria which allow to accurately predict the quality of low-rank approximations computed using randomized sampling. This helps reduce the total number of random samples as well as reduce the communication cost. We apply these adaptive randomized sampling schemes for the construction of hierarchically semi-separable matrices. Compared to previous adaptive randomized HSS compression approaches, our new methods are more rigorous and include both absolute and relative stopping criteria. The numerical examples show faster compression time for the new incremental adaptive strategy compared to previous methods. Randomized numerical linear algebra methods are very interesting from a theoretical standpoint. However, writing robust and efficient, parallel software is far from trivial. In this paper we have focused on a number of practical issues regarding the adaptive compression of HSS matrices, leading to faster compression, with guaranteed accuracy. The methods shown here should carry over to other structured matrix representations.

Acknowledgments. This research was supported in part by the Exascale Computing Project (17-SC-20-SC), a collaborative effort of the U.S. Department of Energy Office of Science and the National Nuclear Security Administration, and in part by the U.S. Department of Energy, Office of Science, Office of Advanced Scientific Computing Research, Scientific Discovery through Advanced Computing (SciDAC) program.

This research used resources of the National Energy Research Scientific Computing Center (NERSC), a U.S. Department of Energy Office of Science User Facility operated under Contract No. DE-AC02-05CH11231.

We thank Guillaume Sylvand (Airbus) for providing us with the BEM test problems. We thank Daniel Haxton (LBNL) and Jeremiah Jones (Arizona State University) for providing us with the Quantum Chemistry test problem.

We thank Yang Liu (LBNL), Wissam Sid Lakhdar (LBNL), and Liza Rebrova (UCLA) for the insightful discussions throughout this research.

Appendix A. Probability Theory. Here, we go through the details of the probability theory mentioned in Section 2.5. We define the random variables

$$(A.1) \quad \begin{aligned} X &\sim \sigma_1^2 \xi_1^2 + \cdots + \sigma_r^2 \xi_r^2 \\ \bar{X}_d &\sim \frac{1}{d} [X_1 + \cdots + X_d], \end{aligned}$$

where $\xi_j \sim \mathcal{N}(0,1)$, $\sigma_1 \geq \cdots \geq \sigma_r > 0$ are the singular values of A , and X_i are independent realizations of X . Clearly $\mathbb{E}(X) = \mathbb{E}(\bar{X}_d) = \|A\|_F^2$.

We prove the following probabilistic bounds:

$$(A.2) \quad \begin{aligned} \mathbb{P} \left[\bar{X}_d \geq \|A\|_F^2 \tau \right] &\leq \exp \left(-\frac{d\tau}{2} \right) \|A\|_F^{dr} \prod_{k=1}^r (A'_k)^{-d} & \tau > 1 \\ \mathbb{P} \left[\bar{X}_d \leq \|A\|_F^2 \tau \right] &\leq \exp \left(\frac{d\tau}{2} \right) \|A\|_F^{dr} \prod_{k=1}^r (A''_k)^{-d} & \tau \in [0, 1), \end{aligned}$$

where

$$(A.3) \quad \begin{aligned} \|A\|_F^2 &= \sigma_1^2 + \cdots + \sigma_r^2 \\ (A'_k)^2 &= \|A\|_F^2 - \sigma_k^2 \\ (A''_k)^2 &= \|A\|_F^2 + \sigma_k^2. \end{aligned}$$

We will show particular realizations of the random variable deviate from the mean with exponentially-decaying probability and gives an accurate way to estimate $\|A\|_F$ using random (Gaussian) samples of the range. Thus, the new stopping criterion accurately estimates the error; the singular values determine the exact exponential-decaying probability.

A.1. Chernoff's Inequality. We use the following theorem [2]:

THEOREM A.1 (Chernoff's Inequality). *Given a random variable X , we have*

$$(A.4) \quad \mathbb{P}[X \geq a] \leq \min_{t>0} e^{-ta} \mathbb{E}(e^{tX}).$$

Here, $\mathbb{E}(e^{tX})$ is the moment generating function of a random variable X . A slight modification of Theorem A.1 gives

$$(A.5) \quad \mathbb{P}[X \leq a] \leq \min_{t>0} e^{ta} \mathbb{E}(e^{-tX}).$$

X is merely linear combinations of chi-squared distributions, so by using properties of the moment generating function we see

$$(A.6) \quad M_{\bar{X}_d}(t) = \prod_{k=1}^d \left(1 - \frac{2\sigma_k^2 t}{d}\right)^{-\frac{d}{2}}.$$

Unfortunately, it is difficult to compute

$$(A.7) \quad \min_{t>0} e^{-ta} M_{\bar{X}_d}(t)$$

analytically, as it reduces to computing the zeros of a degree r polynomial. Instead, we settle for choosing a particular value of t . Setting

$$(A.8) \quad \bar{t} = \frac{d}{2\|A\|_F^2}$$

and $a = \|A\|_F^2 \tau$, with $\tau > 1$, we find

$$(A.9) \quad \mathbb{P}[\bar{X}_d \geq \|A\|_F^2 \tau] \leq \exp\left(-\frac{d\tau}{2}\right) \|A\|_F^{dr} \prod_{k=1}^r (A'_k)^{-d} \quad \tau > 1,$$

where A'_k is defined in Eq. (A.3). In a similar manner, we can obtain a lower bound

$$(A.10) \quad \mathbb{P}[\bar{X}_d \leq \|A\|_F^2 \tau] \leq \exp\left(\frac{d\tau}{2}\right) \|A\|_F^{dr} \prod_{k=1}^r (A''_k)^{-d} \quad \tau \in [0, 1).$$

It is clear that these lower bounds are not optimal and more rigorous analysis would produce tighter bounds, but we will not investigate this further. The bounds we just obtained are sufficient for our purposes.

A.2. Exponential Decay. We now work through the details to show we have exponential-decaying tail probabilities once we are far enough away from the expected value. The restrictions are mild: for lower bounds, we require $\tau < \ln 2$; for upper bounds we require $\tau > 1 + \frac{\|A\|_2^2}{\|A\|_F^2 - \|A\|_2^2}$. The probability distributions do not apply for rank-1 matrices (when $\|A\|_2 = \|A\|_F$), but in then Chernoff's Inequality can be used to compute optimal bounds on tail probabilities. Therefore, we ignore this case.

A.2.1. $\mathbb{P} \left[\bar{X}_d \geq \|A\|_F^2 \tau \right]$. For $\tau > 1$, we have

$$\begin{aligned} \mathbb{P} \left[\bar{X}_d \geq \|A\|_F^2 \tau \right] &\leq \exp \left(-\frac{d\tau}{2} \right) \|A\|_F^{dr} \prod_{k=1}^r (A'_k)^{-d} \\ (A.11) \qquad \qquad \qquad &= \exp \left[\frac{d}{2} \{(\nu_1 + \dots + \nu_r) - \tau\} \right], \end{aligned}$$

where

$$(A.12) \qquad \qquad \qquad \nu_k = \ln \left[\frac{1}{1 - \frac{\sigma_k^2}{\|A\|_F^2}} \right].$$

To have exponential decay in probability, we require

$$(A.13) \qquad \qquad \qquad \nu_1 + \dots + \nu_r < \tau.$$

Because $-\ln x$ is convex on $(0, \infty)$, we see that for $\alpha \in (0, 1)$, we have

$$(A.14) \qquad \qquad \ln \left(\frac{1}{1-x} \right) \leq \frac{x}{\alpha} \ln \left(\frac{1}{1-\alpha} \right) \quad x \in [0, \alpha].$$

Now, we know $\frac{\sigma_k^2}{\|A\|_F^2} \leq \frac{\|A\|_2^2}{\|A\|_F^2}$, so we let

$$(A.15) \qquad \qquad \qquad \alpha = \frac{\|A\|_2^2}{\|A\|_F^2}.$$

Combing this with the fact that $\ln(1+x) \leq x$, we see

$$\begin{aligned} \nu_1 + \dots + \nu_r &\leq \frac{\sigma_1^2}{\|A\|_F^2} \frac{1}{\alpha} \ln \left(\frac{1}{1-\alpha} \right) + \dots + \frac{\sigma_r^2}{\|A\|_F^2} \frac{1}{\alpha} \ln \left(\frac{1}{1-\alpha} \right) \\ (A.16) \qquad \qquad \qquad &\leq \frac{1}{1-\alpha}. \end{aligned}$$

If we plug in α from Eq. (A.15), we see that we require

$$(A.17) \qquad \qquad \qquad \tau > 1 + \frac{\|A\|_2^2}{\|A\|_F^2 - \|A\|_2^2}$$

in order to have exponentially decaying tail probabilities in d .

A.2.2. $\mathbb{P} \left[\bar{X}_d \leq \|A\|_F^2 \tau \right]$. For $\tau \in [0, 1)$, we have

$$\begin{aligned} \mathbb{P} \left[\bar{X}_d \leq \|A\|_F^2 \tau \right] &\leq \exp \left(\frac{d\tau}{2} \right) \|A\|_F^{dr} \prod_{k=1}^r (A''_k)^{-d} \\ (A.18) \qquad \qquad \qquad &= \exp \left[\frac{d}{2} \{ \tau - (\lambda_1 + \dots + \lambda_r) \} \right], \end{aligned}$$

where

$$(A.19) \qquad \qquad \qquad \lambda_k = \ln \left[1 + \frac{\sigma_k^2}{\|A\|_F^2} \right].$$

To have exponential decay in probability, we require

$$(A.20) \quad \lambda_1 + \cdots + \lambda_r > \tau.$$

Now, we know

$$(A.21) \quad \ln(1+x) \geq x \ln 2 \quad x \in [0, 1],$$

so this implies

$$(A.22) \quad \begin{aligned} \lambda_1 + \cdots + \lambda_r &\geq \frac{\sigma_1^2}{\|A\|_F^2} \ln 2 + \cdots + \frac{\sigma_r^2}{\|A\|_F^2} \ln 2 \\ &= \ln 2. \end{aligned}$$

Therefore, so long as $\tau < \ln 2$, we have exponentially decaying tail probabilities in d .

REFERENCES

- [1] L. S. BLACKFORD, J. CHOI, E. D’AZEVEDO, J. DEMMEL, I. DHILLON, J. DONGARRA, S. HAMMARLING, G. HENRY, A. PETITET, K. STANLEY, D. WALKER, AND R. C. WHALEY, *ScaLAPACK Users’ Guide*, SIAM, Philadelphia, 1997.
- [2] P. BRÉMAUD, *Discrete Probability Models and Methods: Probability on Graphs and Trees, Markov Chains and Random Fields, Entropy and Coding*, Probability Theory and Stochastic Modelling, Springer International Publishing, 2017.
- [3] S. CHANDRASEKARAN, M. GU, AND W. LYONS, *A fast adaptive solver for hierarchically semiseparable representations*, CALCOLO, 42 (2005), pp. 171–185.
- [4] J. DEMMEL, L. GRIGORI, M. HOEMMEN, , AND J. LANGOU, *Communication-optimal Parallel and Sequential QR and LU Factorizations*, SIAM Journal on Scientific Computing, 34 (2012), pp. A206–A239.
- [5] P. GHYSELS, X. S. LI, C. GORMAN, AND F.-H. ROUET, *A robust parallel preconditioner for indefinite systems using hierarchical matrices and randomized sampling*, in Parallel and Distributed Processing Symposium (IPDPS), 2017 IEEE International, IEEE, 2017, pp. 897–906.
- [6] P. GHYSELS, X. S. LI, F.-H. ROUET, S. WILLIAMS, AND A. NAPOV, *An efficient multi-core implementation of a novel hss-structured multifrontal solver using randomized sampling*, SIAM Journal on Scientific Computing, 38 (2016), pp. 358–384.
- [7] M. GU AND S. C. EISENSTAT, *Efficient algorithms for computing a strong rank-revealing QR factorization*, SIAM Journal on Scientific Computing, 17 (1996), pp. 848–869.
- [8] W. HACKBUSCH AND S. BÖRM, *Data-sparse Approximation by Adaptive \mathcal{H}^2 -Matrices*, Computing, 69 (2002), pp. 1–35.
- [9] W. HACKBUSCH AND B. N. KHOROMSKIJ, *A sparse h-matrix arithmetic.*, Computing, 64 (2000), pp. 21–47.
- [10] N. HALKO, P. G. MARTINSSON, AND J. A. TROPP, *Finding structure with randomness: probabilistic algorithms for constructing approximate matrix decompositions*, SIAM Rev., 53 (2011), pp. 217–288.
- [11] X. LIU, J. XIA, AND M. V. DE HOOP, *Parallel randomized and matrix-free direct solvers for large structured dense linear systems*, SIAM Journal on Scientific Computing, 38 (2016), pp. S508–S538.
- [12] P.-G. MARTINSSON, *A fast randomized algorithm for computing a hierarchically semiseparable representation of a matrix*, SIAM Journal on Matrix Analysis and Applications, 32 (2011), pp. 1251–1274.
- [13] Å. BJÖRCK, *Numerics of gram-schmidt orthogonalization*, Linear Algebra and its Applications, 197–198 (1994), pp. 297 – 316.
- [14] F.-H. ROUET, X. S. LI, P. GHYSELS, AND A. NAPOV, *A distributed-memory package for dense Hierarchically Semi-Separable matrix computations using randomization*, ACM Transactions on Mathematical Software, 42 (2016).
- [15] G. STEWART, *Block Gram-Schmidt Orthogonalization*, SIAM Journal on Scientific Computing, 31 (2008), pp. 761–775.
- [16] R. A. VAN DE GELIJN AND J. WATTS, *SUMMA: Scalable universal matrix multiplication algorithm*, Concurrency Practice and Experience, 9 (1997), pp. 255–274.

- [17] J. VOGEL, J. XIA, S. CAULEY, AND V. BALAKRISHNAN, *Superfast divide-and-conquer method and perturbation analysis for structured eigenvalue solutions*, SIAM Journal on Scientific Computing, 38 (2016), pp. A1358–A1382.
- [18] Y. XI AND J. XIA, *On the stability of some hierarchical rank structured matrix algorithms*, SIAM Journal on Matrix Analysis and Applications, 37 (2016), pp. 1279–1303.
- [19] Y. XI, J. XIA, S. CAULEY, AND V. BALAKRISHNAN, *Superfast and stable structured solvers for toeplitz least squares via randomized sampling*, SIAM Journal on Matrix Analysis and Applications, 35 (2014), pp. 44–72.
- [20] J. XIA, S. CHANDRASEKARAN, M. GU, AND X. S. LI, *Superfast multifrontal method for large structured linear systems of equations*, SIAM Journal on Matrix Analysis and Applications, 31 (2010), pp. 1382–1411.